COBEM 99
XV Congresso Brasileiro de Engenharia Mecânica
15th Brazilian Congress of Mechanical Engineering
22 - 26 de Novembro de 1999 / November 22 - 26, 1999 Águas de Lindóia, São Paulo,

EXCITATION, PROPAGATION, AND DETECTION OF STRUCTURAL WAVES IN PIEZOELECTRIC COMPOSITE BEAMS

Antonio Lopes Gama
Universidade Federal Fluminense, Departamento de Engenharia Mecânica
24210-000, Niterói, RJ
Arthur M. B. Braga
Sergio K. Morikawa
Luís P. F. de Barros
PUC-Rio, Departamento de Engenharia Mecânica
22453-900, Rio de Janeiro, RJ

Abstract *A model based on Reddy's discrete layerwise laminate theory is employed to simulate the high-frequency (short-wavelength) excitation, propagation, and sensing, of structural waves in composites containing piezoelectric sensors and actuators. Comparisons between approximate and exact wave dispersion spectra are performed in order to assess the efficiency of the layerwise theory in the high-frequency range. A study of the propagation of guided waves in an 11-ply ARALL beam with bonded PZT layers is reported. It is shown that, by employing the appropriate interpolation scheme, the approximate model is capable of reproducing the exact dispersion spectrum at wavelengths to thickness ratios as low as* $\lambda/h = 0.25$. *Finally, results from simulations of the broadband, frequency response of an active aluminum beam with simulated defects of different depths are presented and compared with data from similar experiments.*

Keywords: *Smart Structures, Piezoelectric Sensors and Actuators, Wave Propagation*

1. INTRODUCTION

The electromechanical behavior of piezoelectric laminates has been extensively studied in the past few years. Most of the studies to date have been concerned with vibration and structural acoustic control, where the dynamic response is within the modal domain. Few attempts have been made to evaluate the effectiveness of available laminate models in the high-frequency range. The present contribution addresses the problem of modeling the excitation, propagation, and sensing, of high-frequency (short-wavelength) structural waves in composites containing piezoelectric sensors and actuators. Potential applications are related with health monitoring and damage detection in composite structures. As schematically depicted in Figure 1, piezoelectric

actuators may be employed to launch guided waves which, after interacting with structural defects such as voids, cracks, or delaminations, are sensed by the same or other piezoelectric elements, also bonded or embedded in the composite. Efforts towards the development of this approach to health monitoring have been recently reported by Monkhouse *et al.* (1998), Badcock and Birt (1998), and Lin and Chang (1999).

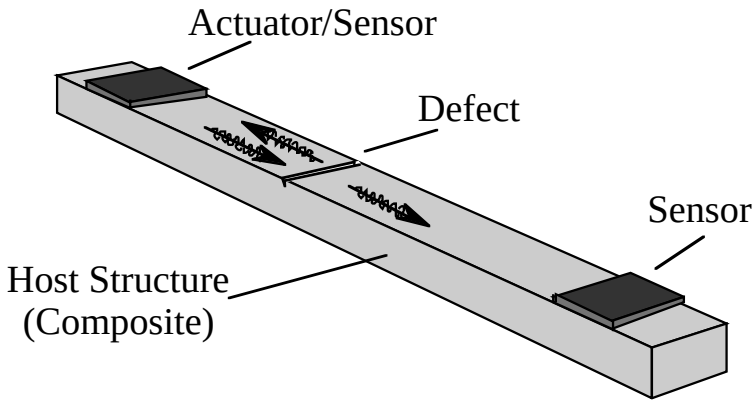

Figure 1: Health monitoring using bonded piezoelectric sensors and actuators

The resolution of this on-board, non destructive evaluation tool increases as the wavelengths of the guided waves in the structure become shorter. In the case of slender elements, such wavelengths may be much smaller than the structure's thickness. At this high-frequency range, the well-known models for the excitation and sensing of bonded or embedded piezoelectric patches, often based on static equivalent forces or bending moments, are no longer accurate (Braga *et al.*, 1998; de Barros, 1998). Simulations of the interactions between sensors/actuators and the host structure must now take into account the coupled electromechanical equations. Furthermore, at this short-wavelength range, classical as well as some of the higher order shear deformation laminate theories fail to accurately represent the dynamic response of the slender composite structure (Braga *et al.*, 1998). Finite element simulations must also be employed with caution, since very thin meshes are needed to capture the rapidly varying oscillating fields (Gama, 1998; de Barros, 1998).

The model for the active composite beam proposed here is based on Reddy's layerwise laminate theory (Robbins and Reddy, 1991; Reddy, 1993; Robbins and Reddy, 1994; Lee and Saravanos, 1997). The displacement and electric potential are interpolated in the through-thickness direction using piecewise linear functions. In the frequency domain, the governing equations are written in a state space form. Comparisons between approximate and exact wave dispersion spectra are performed in order to assess the efficiency of the layerwise theory in a given frequency range. It is shown that by employing the proper interpolation, Reddy's theory is able to describe the dynamic response of the composite at frequencies where the associated wavelengths are of the same order or even shorter than the thickness of the anisotropic and/or piezoelectric layers. This is verified in a study of the dispersion spectrum of guided waves propagating in an composite beam with PZT layers bonded to its surface.

In the case of a beam with abrupt changes in thickness, introduced in order to simulate structural defects, the solution for the state space equation is obtained by em-

ploying an algorithm based on a discrete version of the Riccati transformation (Gama, 1998; de Barros, 1998). Results from evaluations of the broad-band, frequency response of an active aluminum beam with simulated defects of different depths are presented, and compared with data from similar experiments. Despite the number of simplifications used in the approximate model, the qualitative agreement between numerical and experimental results is quite satisfactory. In addition, it is verified that, as one might expect, the influence of the defect depth on the sensor response increases with the frequency of the acoustic signal. It is also shown that placing the piezoelectric sensor near the simulated defect, sharply improves its ability to sense changes in size of the defect.

2. MODEL FOR LAMINATED PIEZOELECTRIC BEAMS

We employ Reddy's layerwise theory (Reddy and Robbins, 1994) to describe the response of laminate piezoelectric beams. This approximate theory is based on the following assumed, through-thickness, distributions of the displacement field:

$$u_x(x,z,t) = \sum_{\alpha=1}^{N} \xi^{\alpha}(z)\, U_{\alpha}(x,t) \quad \text{and} \quad u_z(x,z,t) = \sum_{\beta=1}^{M} \xi^{\beta}(z)\, W_{\beta}(x,t) \tag{1}$$

and of the electric potential:

$$\phi(x,z,t) = \sum_{\gamma=1}^{P} \xi^{\gamma}(z)\, V_{\gamma}(x,t) \tag{2}$$

Although in Reddy's Layerwise Theory the degree and number of the interpolation functions $\xi^{\alpha}(z)$, are arbitrary, we are employing in this paper only linear, Lagrange polynomials. The number of polynomials is equal to the number of layers plus one, that is, we take $\alpha, \beta, \gamma = 1, 2, \ldots, n, n+1$, where n is the number of layers in the laminate. Hence U_{α} and W_{α} are, respectively, the in-plane and transverse displacements at the interface between the layers $\alpha-1$ and α. Accordingly, V_{α} represents the electric potential on the same interface. We may, arbitrarily, increase the number of linear interpolation polynomials by subdividing the homogeneous layers in thinner sublayers, with the same material properties as the original ones.

Generalized forces and charges are defined as (Braga, *et al.*, 1998, Gama, 1998):

$$N_I^{\alpha} = \int_{\mathcal{R}} T_I\, \xi^{\alpha}\, dA, \quad \text{and} \quad j^{\alpha} = \int_{\mathcal{R}} D_1\, \xi^{\alpha}\, dA, \tag{3}$$

where $I = 1, 3, 5$, and $\mathcal{R}$ is the beam's cross-section, while T_I represents the stress components and D_x the electric displacement in the x direction.

In the model, it is also important to make a distinction between those interfaces with or without electrodes. Since the electric potential is uniform at the perfectly conductive electrodes, we let

$$\frac{\partial V_{\alpha}^{e}}{\partial x} = 0 \tag{4}$$

at the electroded interfaces, identified by the label e. Also, due to the current flowing through the electrode and its electric connection, the transverse component of the electric displacement may experience a jump, which is equal to the surface charge density at that interface. Furthermore, if the electrode belongs to an actuating lamina, V_α^e is given, and q_α^e is not known. If, on the other hand, the electrode is placed on a sensor, one may consider two measurement configurations. In the first, the electric charge, or current, is the measured quantity, $V_\alpha^e = 0$ (short-circuit), and q_α^e is the unknown variable that must be integrated over the length of the electrode to yield the sensor output. On the other hand, if voltage across the piezoelectric layer is being measured, we set $q_\alpha^e = 0$ (open-circuit) and then solve the governing equations to evaluate V_α^e, the sensor response. In yet another sensor configuration, not explicitly considered here, one may take into account the impedance of the measurement circuit by introducing a linear relationship between the voltage and the electric current (Carpenter, 1997).

On the non electroded interfaces, such as those between sublayers introduced to refine the through-thickness interpolation, the potential is not necessarily uniform, and the electric displacement must be continuous, hence:

$$q_\alpha^o = 0 \tag{5}$$

where the label o is used to identify those interfaces.

It may be shown that by applying Reddy's approximation in the variational formulation for piezoelectric media, the set of equations governing the time-harmonic response of piezoelectric composite beams may be cast in the following matrix form (Braga *et al.*, 1998; Gama, 1998; de Barros, 1998):

$$\frac{d\boldsymbol{\zeta}}{dx} = \boldsymbol{\mathcal{M}}\,\boldsymbol{\zeta} + \boldsymbol{\mathcal{H}}\,\boldsymbol{V}^e \quad \text{and} \quad \boldsymbol{q}^e = \boldsymbol{\mathcal{S}}\,\boldsymbol{\zeta} + \boldsymbol{\mathcal{P}}\,\boldsymbol{V}^e \tag{6}$$

with the state vector, $\boldsymbol{\zeta}$, defined as:

$$\boldsymbol{\zeta}^T = \begin{bmatrix} \boldsymbol{U} & \boldsymbol{W} & \boldsymbol{V}^o & \boldsymbol{N}_1 & \boldsymbol{N}_5 & \boldsymbol{j}_o \end{bmatrix} \tag{7}$$

where $\boldsymbol{U}$, $\boldsymbol{W}$, $\boldsymbol{N}_1$, and $\boldsymbol{N}_5$ are vectors of dimension $n+1$ grouping, respectively, the variables U_α, W_α, N_1^α, and N_5^α. The dimension of vectors $\boldsymbol{V}^e$, $\boldsymbol{q}^e$, $\boldsymbol{V}^o$ and $\boldsymbol{j}_o$, respectively grouping V_α^e, q_α^e, V_α^o, and j_o^α, will depend on the number of interfaces with and without electrodes. Matrices $\boldsymbol{\mathcal{M}}$, $\boldsymbol{\mathcal{H}}$, $\boldsymbol{\mathcal{S}}$, and $\boldsymbol{\mathcal{P}}$, whose components have been omitted here due to the lack of space, depend on the mechanical, piezoelectric, and dielectric material constants (Gama, 1998; de Barros, 1998).

The first of Eqs. (6) describes the time-harmonic response of the piezoelectric beam to the imposed electric potential $\boldsymbol{V}^e$. The second, relates the electric charge on the electrodes with the other field variables. When one of the layers is used as a charge sensor we simulate its response by, as pointed out above, letting the electric potential be equal to zero on its surfaces, and, through the second equation of (6), evaluating the resulting electric charges. Equations (6) must be slightly modified when the layer is employed as a voltage sensor. Details of this modifications are also omitted here due to lack of space (Gama, 1998).

3. WAVE DISPERSION ANALYSIS

In this section, we present a study of the dispersion spectrum of the guided wave-modes that propagate along an 11-ply beam made of ARALL, which is a composite fabricated from alternate layers of alluminum and uniderctional, fiber reinforced, aramide-epoxi laminae. In addition, the beam has piezoceramic (PZT) layers on its top and bottom surfaces. Both the aluminum and the aramide-epoxi layers are 1 mm-thick. The thickness of the PZT layers are 2 mm. Mechanical, piezoelectric, and dielectric properties of alluminum, aramide-epoxi, as well as for the piezoceramic material considered in this study, may be found in (Gama, 1998).

In the wave dispersion analysis presented here, the piezoelectric layers were assumed to be short-circuited. Dispersion curves, which relate the wavenumber of the guided modes with the frequency, are constructed by applying the approximate model described above as well as by solving the equations governing the electroelastic dynamic response of the layered piezoelectric solid. Details of the algorithm employed to obtain the exact dispersion curves may be found in (Braga *et al.*, 1992; Gama, 1998).

The approximate dispersion curves are obatined by observing that for a short-circuited beam, the vector $\boldsymbol{V}^e$ in equation (6) vanishes. Hence, one has

$$\frac{d\boldsymbol{\zeta}}{dx} = \boldsymbol{\mathcal{M}}\,\boldsymbol{\zeta} \tag{8}$$

For an infinite beam, $\boldsymbol{\mathcal{M}}$ is uniform, and therefore the solution of (8) is

$$\boldsymbol{\zeta}(x) = \sum_{j=1}^{n+1} a_j\,\boldsymbol{\zeta}_j\,e^{\alpha_j x} \tag{9}$$

where α_j and $\boldsymbol{\zeta}_j$ are the eigenvalues and eigenvectors of the state matrix $\boldsymbol{\mathcal{M}}$, while a_j are constants, and n is the number of layers employed in the approximate model. Each term in the sum may be associated with one guided mode in the beam. Imaginary values of α_j represent traveling waves, whereas those eigenvalues with nonvanishing real part are related to evanescent modes. It should be pointed out that the state matrix has the following property (Gama, 1998):

$$\boldsymbol{T}\boldsymbol{\mathcal{M}}\boldsymbol{T}^T = -\boldsymbol{\mathcal{M}}^T\ , \quad \text{where} \quad \boldsymbol{T} = \begin{bmatrix} 0 & \boldsymbol{I} \\ -\boldsymbol{I} & 0 \end{bmatrix} \tag{10}$$

where $\boldsymbol{I}$ is the identity matrix. It may be shown that, as a consequence of (10), the eigenvalues of $\boldsymbol{\mathcal{M}}$ appear in pairs of opposite signs. This simply expresses the fact that the guided modes propagate with the same wave speed, or, in the case of evanescent waves, are equally attenuated, in both directions of the x-axis.

A plot of both the exact and approximate dispersion spectra for the ARALL/PZT beam is shown in Figure 2. Only the travelling wave-modes, *i.e.*, those for which the eigenvalue α_j is imaginary, are represented. The matching between exact and approximate dispersion curves is very good, even for modes with wavelength to thickness ratios as low as $\lambda/h = 0.25$.

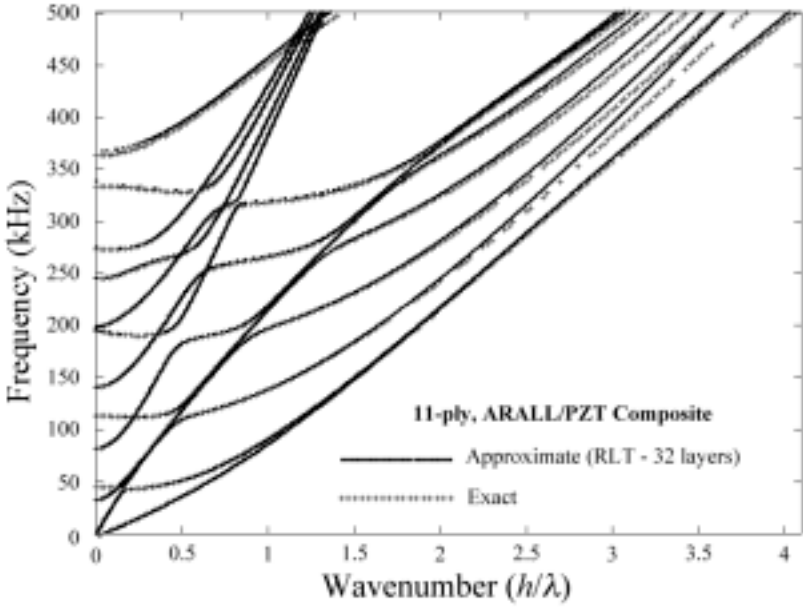

Figure 2: Dispersion spectrum for a 15 mm-thick ARALL/PZT beam.

In Figures 3 and 4, we present through-thickness distributions of the displacement and electric potential fields for two guided wave-modes that may propagate freely in the composite beam. In both cases, even though the wavelengths are shorter than the beam thickness, the agreement between the exact and approximate solutions is very good. In Figure 3, at 36 kHz and $\lambda/h = 2$, it is interesting to observe the zigzag-like distribution of the in-plane displacement, typical of the medium frequency range for this composite with alternating layers of materials with very dissimilar shear moduli. It is then clear that other laminate theories, such as the Classical or the First Order Shear Deformation, that assume linear through-thickness distributions of the in-plane displacement, are unable to represent the dynamic response of the ARALL/PZT beam at this frequency range. Regarding Figure 4, representing a guided mode that, at 501 kHz, has a wavelength which is one fourth of the beam thickness, one notices that the wave profile is typical of a surface wave. Indeed, we observe that the fields decay very rapidly away from the beam's top and bottom surfaces. It should be pointed out, however, that at this short wavelength range, the interpolation in the layerwise theory must be refined in order to capture those sharp gradients in the displacement field. In this case, we have employed 53 piecewise interpolation functions.

4. ANALYSIS OF AN ACTIVE BEAM WITH SIMULATED DEFECTS

Results of a frequency response analysis of an aluminum beam with simulated defects is presented in this section. Both experimental and numerical data are reported. The beam, as shown schematically in Figure 5, is instrumented with 0.5 mm-thick piezoceramic patches that may act as either sensors or actuators. In this case, modeling through the layerwise approximate theory has to take into account that the thickness as well as the mechanical, piezoelectric, and dielectric properties of the beam change along its length. Therefore, as noted elsewhere (Braga *et al.*, 1998; Gama, 1998; de Barros, 1998), the state matrices in equations (6) vary with x in a piece-wise constant fashion. The electromechanical response is then evaluated by employing an algorithm based on the invariant imbedding technique (Dieci, 1992; Gama, 1998). Details of the solution

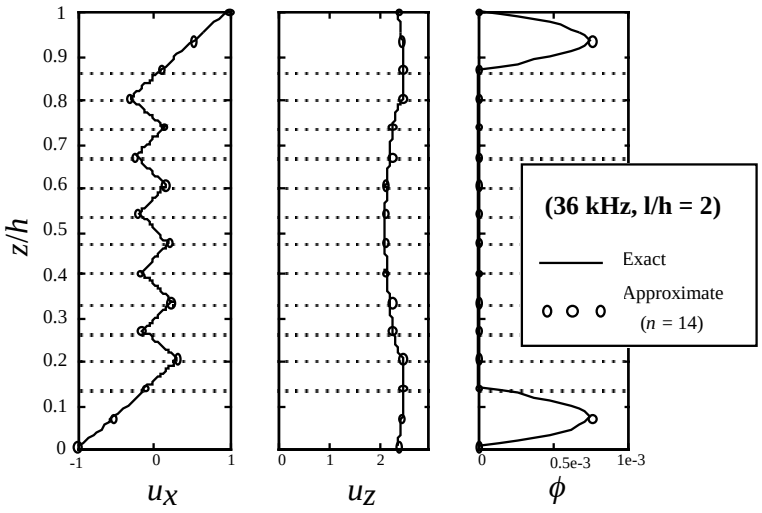

Figure 3: Through-thickness distribution of displacement and electric potential fields.

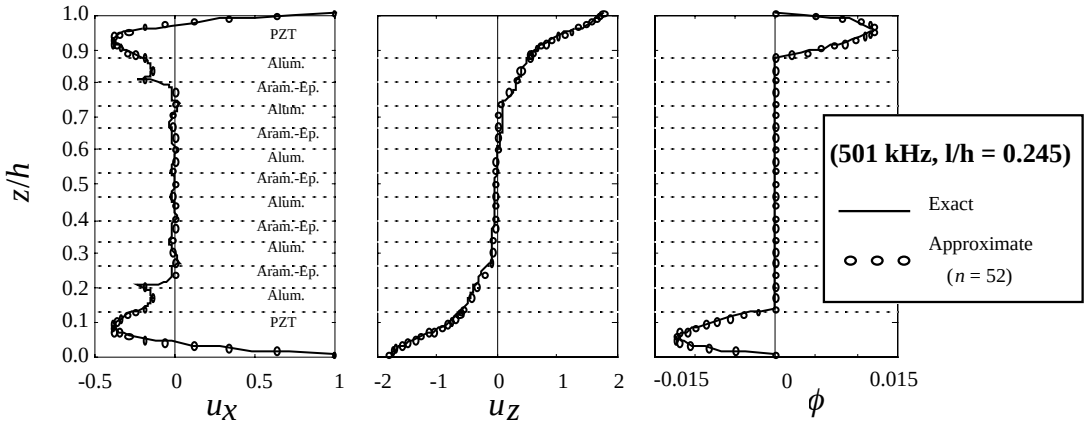

Figure 4: Through-thickness distribution of displacement and electric potential fields.

scheme are omitted here due to the lack of space.

Figure 5 also showns a sketch of the experimental setup employed in a series of measurements of the response of the active beam. The piezoelectric actuators were excited with white noise signals in a frequency range from DC to 12.8 kHz. In all tests the beam was suspended by nylon wires and therefore a free-free boundary condition was assumed in the simulations. Dfects simulating surface breaking cracks were introduced in the beam by cutting slots with 1.0 and 0.3 mm-thick saw blades. The depth of the slots varied from zero to 5.5 mm.

Initially, only the central slot, with depth a_1 in the sketch of Figure 5, was cut. Figure 6 shows both numerical and experimental responses measured by sensor S2 for increasing depths of the central slot. The measured quantity in the experiments was the voltage across the sensor. In the numerical simulations, where equation (10) is solved for the active beam, the surface charge density distribution on the sensors electrode, $q(x)$, was used to quantify the beam's response. The electric current is evaluated through the integral

$$I = -i\omega \int_0^L q(x)\, b\, dx \tag{11}$$

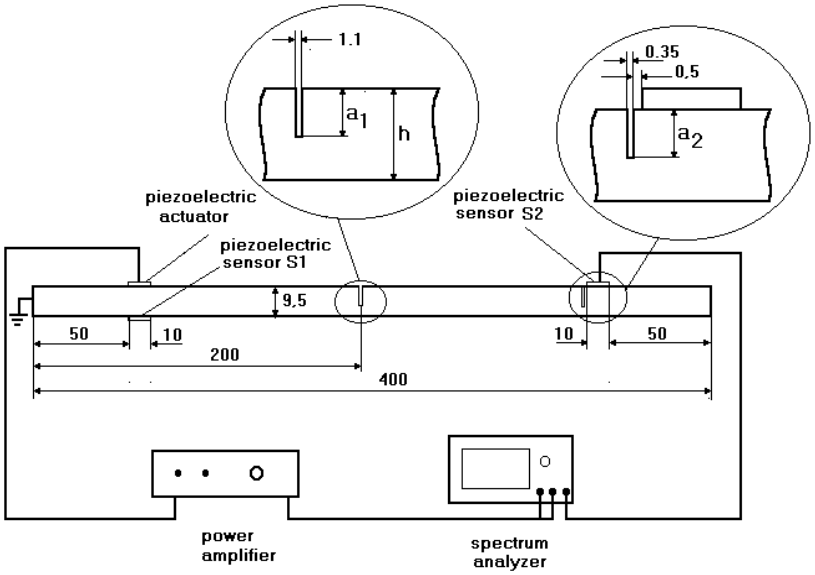

Figure 5: Active aluminum beam and experimetal arrangement (dimensions in mm).

where ω is the angular frequency, L the sensor length, and b the beam width. It should then been pointed out, that, at this point, comparison between numerical and experimental data is only qualitative. At any rate, both results indicate that there is little change in the modal frequency response as the depth to thickness ratio, a_1/h, increases from zero to 0.58.

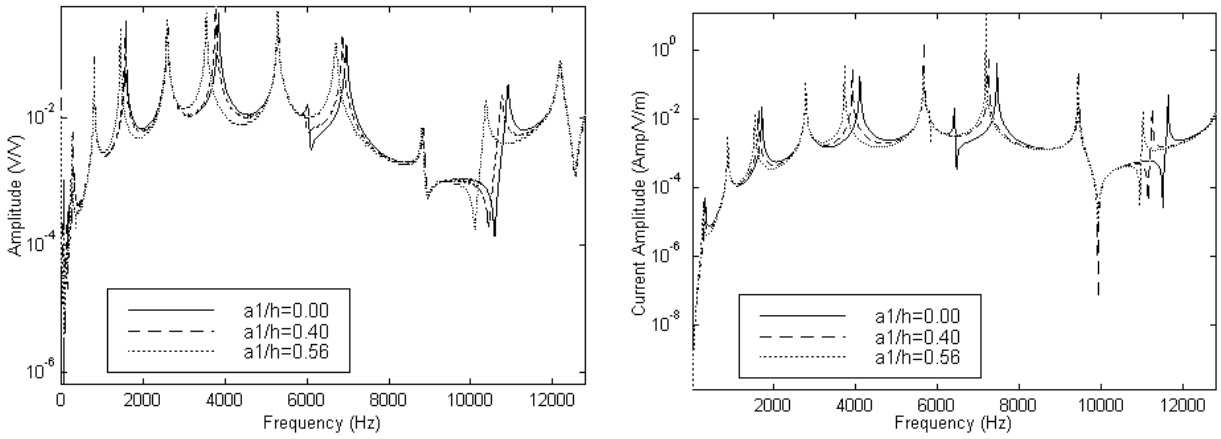

Figure 6: Frequency response for beam with $a_2 = 0$. Experimental (left): voltage on sensor S2; Approximate model(right): electric current on top electrode of S2.

In Figure 7 we present experimental and simulated results for $a_1 = 5.5$ mm and depths of a_2 varying from 0 to 3 mm. Now, the amplitude of the response signal, in particular at frequencies away from the ressonances, is much more sensitive to an increase in the depth of the slot. Figure 8 shows the variation in the measured voltage with the ratio a_2/h at different frequencies. In Figure 9, we present the simulated electric charge distribution in the top electrode of sensor S2, evaluated at 4 kHz as the depth of the slot, a_2, increases from 0.5 to 5 mm.

From this set of results, we conclude that positioning the piezoelectric sensor near the surface breaking defect sharply increases its sensibility to changes in depth, even for frequencies in the modal range. As an outcome, one may conceive a novel method for monitoring the growth of surface breaking defects, where the sensor is positioned

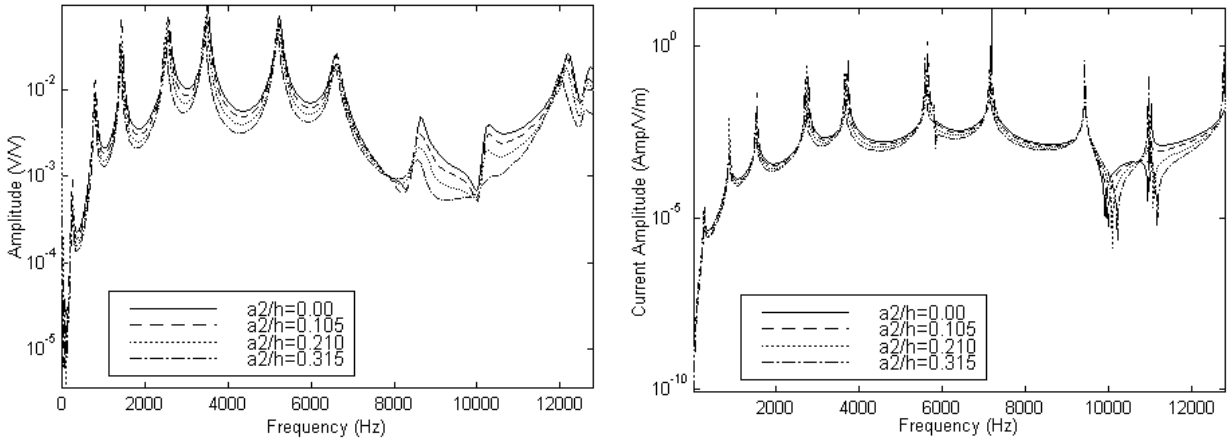

Figure 7: Frequency response for beam with $a_1 = 5.5\,\text{mm}$. Experimental (left): voltage on sensor S2; Approximate model (right): electric current on top electrode of S2.

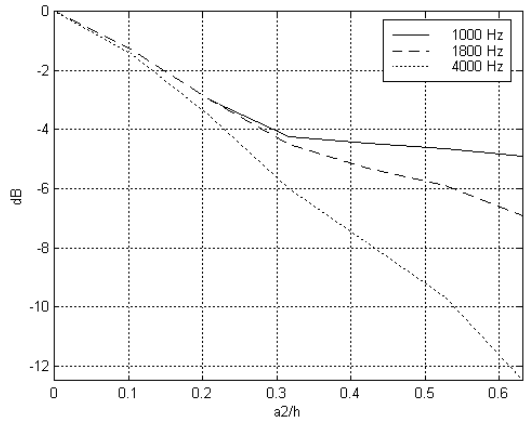

Figure 8: Decay in measured voltage at sensor S2, for different frequencies, as a_2/h increases.

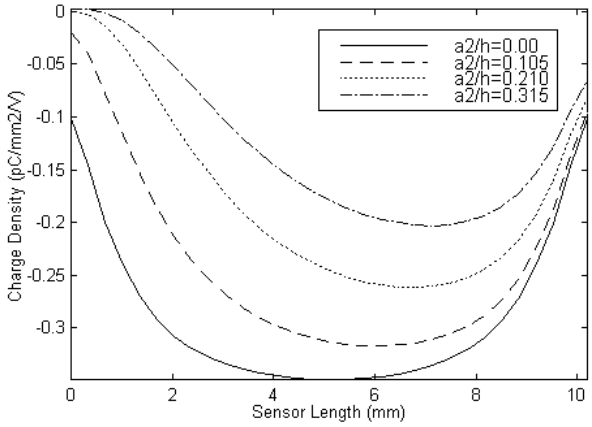

Figure 9: Simulated electric charge distribution on top electrode of S2 as a_2/h increases (4000 Hz).

close to the defect and either broad-band or CW signals are sent from another set of piezoceramic actuators. As demonstrated by the results reported here, this method my be applyed even in the low-frequency (modal) range of the structure. Presently, the authors are conducting a new series of experiments in order to further validate the proposed approach.

5. CONCLUDING REMARKS

In this paper, we have described a model developed to simulate the electromechanical frequency response of laminated piezoelectric composites. The model is based on Reddy's layerwise, laminate theory. It has been verified, by means of comparisons between the exact and approximate dispersion spectra of guided waves, that the model is capable of reproducing the structural response in the high-frequency/short-wavelength range. In particular, if the proper number of interpolation functions is employed, the proposed approach could be applied to model the excitation, propagation, and sensing of surface acoustic waves in the composite beam, where the wavelength to thickness ratio may be as low as 0.25. Results from evaluations of the broad-band, frequency response of an active aluminum beam with surface breaking defects have also been presented, and compared with experimental data. The qualitative agreement between numerical

and experimental results was quite satisfactory. In addition, it has been shown that placing the piezoelectric sensor near the simulated defect, sharply improves its ability to sense changes in the defect's depth.

REFERENCES

Badcock, R. A. and Birt, E. A., 1998, "The use of 0-3 piezocomposite embedded Lamb wave sensors for damage detection in advanced fibre composites", *Proc. of the 4th European Conference on Smart Structures*, Harrogate, UK, July, pp. 373–388.

Braga, A.M.B., Gama, A.L. and de Barros, L.P.F., 1998 "Models for the high frequency response of active piezoelectric composite beams", *Proc. of the 4th European Conference on Smart Structures*, Harrogate, UK, July 6-8, pp115–122.

Braga, A.M.B., Honein,B.,Barbone, P.E. and Herrmann,G., 1992, "Active Suppression of Sound Reflected from a Piezoelectric Plate", *J. of Intell. Mat. Sys. & Struct.*, Vol.3, pp. 209-223.

Carpenter, M.J., 1997, "Using Energy Methods to Derive Beam Finite Elements Incorporating Piezoelectric Materials", *J. of Intell. Mat. Sys. & Struct.*, Vol.8, pp. 26–40.

de Barros, L.P.F., 1998, "Modelagem de Atuadores Piezoelétricos para Vigas Compósitas", Tese de Mestrado, PUC-Rio.

Dieci,L., 1992, "Numerical Integration of the Differential Riccati Equation and Some Related Issues", *SIAM J. Numer. Anal.*, Vol. 29, No 3, pp 781-815.

Gama, A. L., 1998, "Modelagem de Elementos Piezoelétricos para Excitação e Sensoriamento de Sinais Acústicos de Alta Freqüência em Vigas Compósitas," *Tese de Doutorado*, PUC-Rio.

Lee, H. and Saravanos, D.A., 1997, "Generalized Finite Element Formulation for Smart Multilayered Thermal Piezoelectric Composite Plates", *Int. J. Sol. & Struct.*, Vol. 34, No. 6, pp. 355-371.

Lin, M. and Chang, F. K., 1999, "Built-in diagnostics for composite structures", *Proc. of PACAM IV*, Vol. 7, Rio de Janeiro, Brasil, Janeiro, pp. 613–614.

Monkhouse, R.S.C., Wilcox, P.W., Lowe, M.J.S., Dalton, R.P. and Cawley, P., 1998, "The rapid monitoring of structures using interdigital Lamb wave transducers", *Proc. of the 4th European Conference on Smart Structures*, Harrogate, UK, July, pp. 397–404.

Reddy, J. N., 1993, " An evaluation of equivalent-single-layer and layerwise theories of composite laminates", *Composite Structures*, 25 pp 21-35.

Reddy, J. N. and Robbins Jr., D.H., 1994, " Theories an computational models for composite laminates", *Appl. Mech. Rev.* vol 47, No. 6, part 1, pp. 147–169.

Robbins Jr.,D.H. and Reddy, J. N, 1991, "Finite Element Analysis of Piezoelectrically Actuated Beams", *Comput. Struct.*, 41(2), pp. 265-279.